Research Article

The Effect of 60% Cold Rolling on the Microstructure and Mechanical Properties of the High Entropy Alloy AlCoCrFeNi$_{2.1}$

A. Chehri [1], A. Adelkhani[1*] and M. Seifpour Bijnavand [2]

[1] Department of Mechanical Engineering, Kermanshah Branch, Islamic Azad University, Kermanshah, Iran
[2] Department of Materials and Metallurgical Engineering, Amirkabir University of Technology (Tehran Polytechnic), Tehran, Iran

ARTICLE INFO

ABSTRACT

High entropy alloys are a new class of materials that have attracted much attention due to their attractive properties. High entropy alloys have various types and structures, among which, eutectic high entropy alloys have received much attention due to their unique characteristics. In this study, the effect of 60% cold rolling on the properties of AlCoCrFeNi$_{2.1}$ eutectic high entropy alloy is investigated and compared with the casting condition. This alloy shows a layered structure consisting of FCC and BCC phases in both as-cast and cold-alloyed samples. In the as-cast state, the alloy showed a hardness of 352 Vickers, which increased to 401 Vickers following a 60% cold rolling. To further investigate the mechanical properties, both samples were subjected to a shear-punch test (SPT). According to the results, the as-cast sample shows good flexibility and strength which has subsequently risen following cold rolling. The measured values of the yield shear strength and final shear strength for as cast and 60% cold-rolled samples are 204, 269, 294, and 317, respectively.

© Shiraz University, Shiraz, Iran, 2024

1. Introduction

Industrial developments and the need for materials with desirable properties for practical applications have led to many advances in material science. There are many applications for which the desired mechanical and physical properties cannot be easily achieved by traditional alloys [1]. Therefore, due to the increase in demand in various industries, especially in the aerospace, chemical and nuclear industries, many efforts have been made to produce new metal alloys with better mechanical, thermal and chemical properties [1, 2]. The purpose of the development of materials for structural and functional applications is usually to achieve specific mechanical and physical properties such as high strength, good ductility, excellent fracture toughness, suitable creep resistance, high wear resistance, oxidation resistance and good conductivity [3-5]. Different alloys have their

---

advantages and disadvantages, for while example titanium alloys are suitable for low-temperature applications, austenitic steels based on Ni-Cr-Fe are corrosion resistant. Aluminum alloys have low density and low strength, while nickel alloys can be used at high temperatures with high density [5]. Therefore, researchers sought to find new materials that can meet the working conditions in applications and new requirements such as high strength-to-weight ratio, creep strength, and thermal resistance [6]. A different approach emerged in the early 2000s, in which a series of alloys were designed with several major elements and with similar or different atomic percentages. There are at least five main elements in their structures that form a stable solid solution. This stability is due to the high mixing entropy of some elements. These alloys are called high entropy alloys (HEAs) [3]. High entropy alloys include at least 5 main metal elements and compounds whose percentage of elements is in the range of 5-35% and can display a wide range of properties [3, 4]. High entropy alloys have attracted a lot of attention due to their remarkable and unique properties such as high strength and hardness, excellent resistance to corrosion and oxidation, good mechanical properties at high temperature, magnetic properties and remarkable thermal stability. Since the discovery of high entropy alloys, many efforts have been made to understand their concept, and several types of HEA systems with impressive properties have been discovered due to their attractive properties, HEAs serve as new metal alloy systems for high-temperature applications in the aerospace, nuclear, and chemical industries. Multi-phase, refractory, lightweight, amorphous, intermetallic and magnetic HEAs are examples of this type [7].

Compared to conventional alloys, HEAs have four main effects that make them very attractive due to their distinctive properties. These effects are high entropy, strong lattice distortion, slow diffusion and cocktail effect and significantly affect the microstructure and properties of these alloys [8-11]. The high entropy effect as the main concept of HEAs, explains the thermodynamic relations. Strong lattice distortion

affects kinetic properties throughout the phase transformation. The slow permeation effect is an explanation for the effect of low permeation rates on mechanical and chemical properties. Finally, the cocktail effect, which is a separate description for HEAs, has an overall effect on composition, structure, and microstructure properties [8, 10].

It has been found that the phase structure in HEAs can significantly affect their properties and applications [12]. Therefore, an in-depth understanding of the phase structure of HEAs can further help design HEAs with the desired crystal structure. HEAs can exist as solid solutions, intermetallic compounds, amorphous alloys, or a mixture of these phases. Solid solution HEAs are usually composed of BCC, FCC and HCP phases. The phase structures of HEAs are mainly classified into three types according to the number of phases in their microstructure: single-phase HEAs, two-phase HEAs, and amorphous HEAs [13].

Single-phase high entropy alloys with FCC structure show good ductility but lack sufficient strength [14, 15]. On the other hand, single phase HEAs with BCC structure are highly strong, although it makes them extremely brittle [16]. Naturally, one can expect to achieve this balance by using a mix method to obtain an alloy with the combination of both FCC and BCC phases. However, simply introducing a combination of FCC and BCC phases, without proper structural design, cannot solve the problem [17]. In addition, the low castability and segregation of compounds, which are typical for high-entropy alloys, further reduce their mechanical properties and overshadow their engineering applications. To achieve the simultaneous balance of high ductility and strength, it is best to design eutectic alloys with a mixture of soft FCC and hard BCC phases. Eutectic alloys have better castability. Additionally, most importantly, since the eutectic reaction is an isothermal transformation and, hence, there is no solidification temperature range, segregation and shrinkage voids can be reduced. Therefore, eutectic HEAs show good castability and mechanical properties [17-23].

The AlCoCrFeNi$_{2.1}$ eutectic alloy was first introduced by Lee et al., and with a FCC/BCC two-phase structure and a fine and uniform layered microstructure it exhibits a combination of high ductility and fracture toughness [16].

In most of the conducted studies, the properties of this alloy have been investigated after 90% plastic deformation. Therefore, it is not possible to carry out large deformations for various reasons without considering that in some cases there is a need to reduce the cross-sectional area. Hence, this study has been conducted with the aim of investigating the effect of 60% cold rolling on the microstructure and mechanical properties of the AlCoCrFeNi$_{2.1}$ high entropy alloy.

2. Materials and Methods

The production of the AlCoCrFeNi$_{2.1}$ high entropy alloy was carried out using raw materials with 99% purity by arc melting process under argon gas. In this method, a non-consumable tungsten electrode and water-cooled copper bush were used, and before injecting argon into the chamber, a final vacuum of 3×10^{-4} mbar was provided. In order to prepare a homogeneous alloy, the melting process was performed 4 times. The resulting ingot had a thickness of 5 mm. Then it underwent the cold rolling process and reached the desired final thickness of 1.98 mm in 10 passes. For microstructural investigations, samples of primary and cold-rolled alloys were subjected to sanding and polishing operations. Marble solution with the combination of $CuSO_4+HCL+H_2O$ was used to etch the samples. X-ray diffraction (XRD) analysis using Cu K$_\alpha$ radiation in the 2θ range of $30°$-$90°$ was used to characterize the phases present in the initial microstructure.

Surface images of etched samples were taken by electron microscopes. Moreover, the elemental distribution map for the as-cast and cold-rolled samples were prepared and the chemical analysis of different phases was carried out by energy dispersive spectroscopy.

To evaluate the hardness of the samples, a micro hardness device with an applied load of 50 grams in terms of Vickers was used. Hardness was measured for each sample at ten points and then the average hardness was reported. The shear-punch test (SPT) is a simple test to evaluate the mechanical properties in times of limited access to materials and to obtain the yield and ultimate shear strength. Sample preparation for shear-punch test was done according to ASTM D732 standard. The diameter of the mandrel, the cutting matrix and the thickness of the samples in this test were 2.93, 3.32 and 0.6 mm, respectively. The machine speed was selected as 0.3 mm/s. The mandrel applied force to the specimen at a specified strain rate until a flake-shaped specimen was cut from the surface. After that, the shear stress-displacement curve was drawn using the data received from the tension device and from Eq. (1):

$$\tau = \frac{p}{2\pi rt} \tag{1}$$

where τ is the shear stress, p is the applied force, r is the average radius of the punch and die, and t is the thickness of the sample.

3. Results and Discussion

The elements percentage of the high entropy AlCoCrFeNi$_{2.1}$ alloy is shown in Table 1. The results show that Al has the lowest weight percentage among the alloy constituent elements and Ni has the highest. The microstructure of the as-cast AlCoCrFeNi$_{2.1}$ HEA with dendritic/lamellar morphology is shown in Fig. 1 (a and b). In Fig. 1(a), the structure of the alloy including dendrites and eutectic layers can be seen. The thin and long eutectic structures of the high entropy alloy AlCoCrFeNi$_{2.1}$ are evident in the image. The AlCoCrFeNi$_{2.1}$ alloy consists of a soft phase FCC (L12) and a hard phase BCC (B2) with a fine layer structure [16]. As is shown, partitioning of alloying elements between the background and dendritic phases is seen. Analysis of the EDS results revealed that the FCC phase has a high content of Fe, Co and Cr, while

Table 1. The percentage of constituent elements of AlCoCrFeNi$_{2.1}$ alloy

Element	Al	Co	Cr	Fe	Ni
Weight percent	7.6	18.4	17.5	16.7	39.8

the B2 phase is rich in Ni and Al. Table 1 shows the chemical compositions of the different regions marked in Fig. 1 in this alloy. According to the results of Table 2, it can be said that the amount of Al in the areas between the eutectic layers is higher than the background, and the closer we get to the B2 phase, the increase in this value increases. Furthermore, the amount of changes of Cr element in B2 phase is higher than that of Co and Fe elements compared to the L12 phase. In Fig. 1(c), the element distribution map for

the casting sample is shown. In this figure, you can also see the partition between the elements between the phases of this alloy. It is also reported that there are nano-sediments inside the B2 phase. Using transmission electron microscopy, Gao et al. and Shukla et al. showed that the B2 phase also contains nanoscale chromium-rich precipitates in the microstructure of the as-cast alloy [24, 25] According to the results of Table 1, it can be said that points B and D are both B2 phases, but the amount of chromium in point D (16.78% Cr) has increased compared to point B (12.98% Cr), which can be due to the presence of chromium-rich nano-sediments.
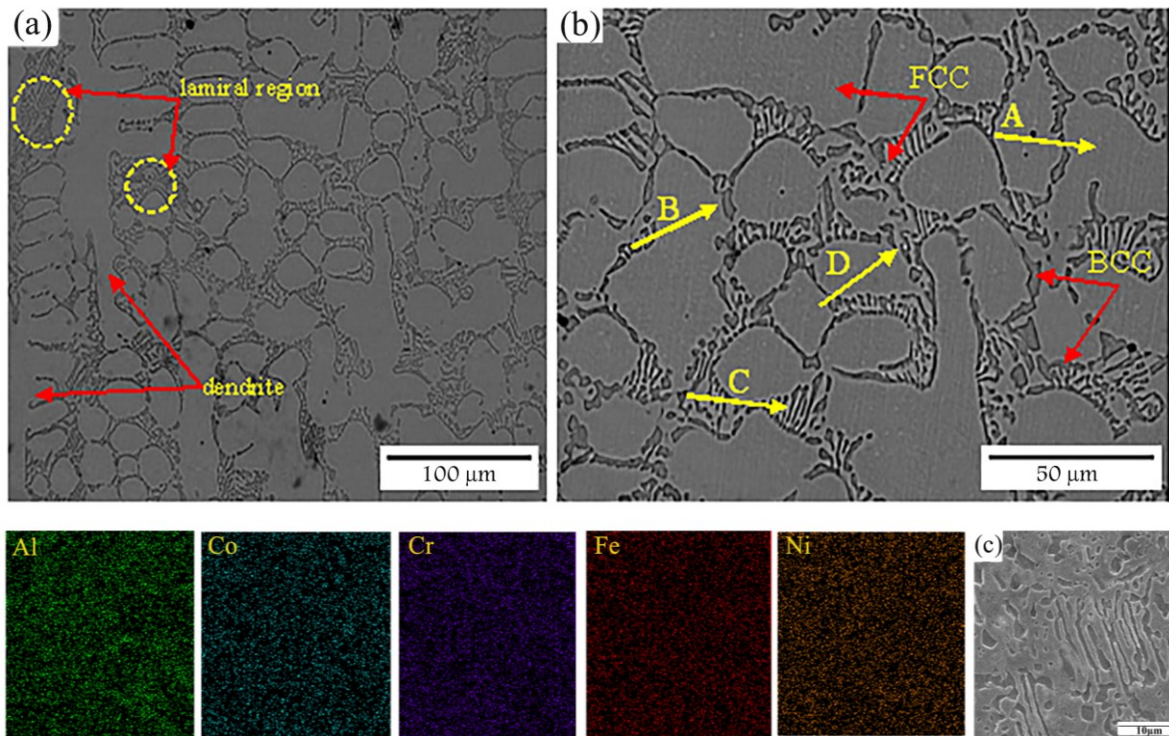
Fig. 1. SEM microstructure image of the (a, b) as-cast AlCoCrFeNi$_{2.1}$ high entropy alloy, and (c) elements distribution map.

Table 2. The results of EDS analysis of the points marked in Fig. 1

Point	Element (wt.%) Al	Co	Cr	Fe	Ni
A	7.62	19.03	18.95	19.55	34.84
B	15.00	15.25	12.98	14.67	42.09
C	10.85	16.81	16.03	16.73	39.58
D	9.68	17.74	16.78	17.58	38.22

Fig. 2 shows the electron microscope image of the alloy after 60% cold rolling. As can be seen, a part of the dendritic structure has been destroyed after the cold rolling process and the B2 phase particles are scattered irregularly and with different sizes in the matrix. As in the as-cast sample, the difference in the percentage of the constituent elements of the phases is obvious. According to the EDS results obtained from different areas of Fig. 2, it can be said that there is no significant difference in terms of the distribution of elements in both L12 and B2 phases in the cooled rolled sample with that of the as-cast sample. In the element distribution map, it can be seen that in some areas, the amount of Cr, Co and Fe elements is larger, and these areas are more abundant and in other areas, which respectively represent L12 and B2 phases, they are empty or very little. There is also this difference in distribution for Al and Ni elements, which is more noticeable for the Al element. In addition, as shown in the figure, phase B2 is aligned with the rolling direction.
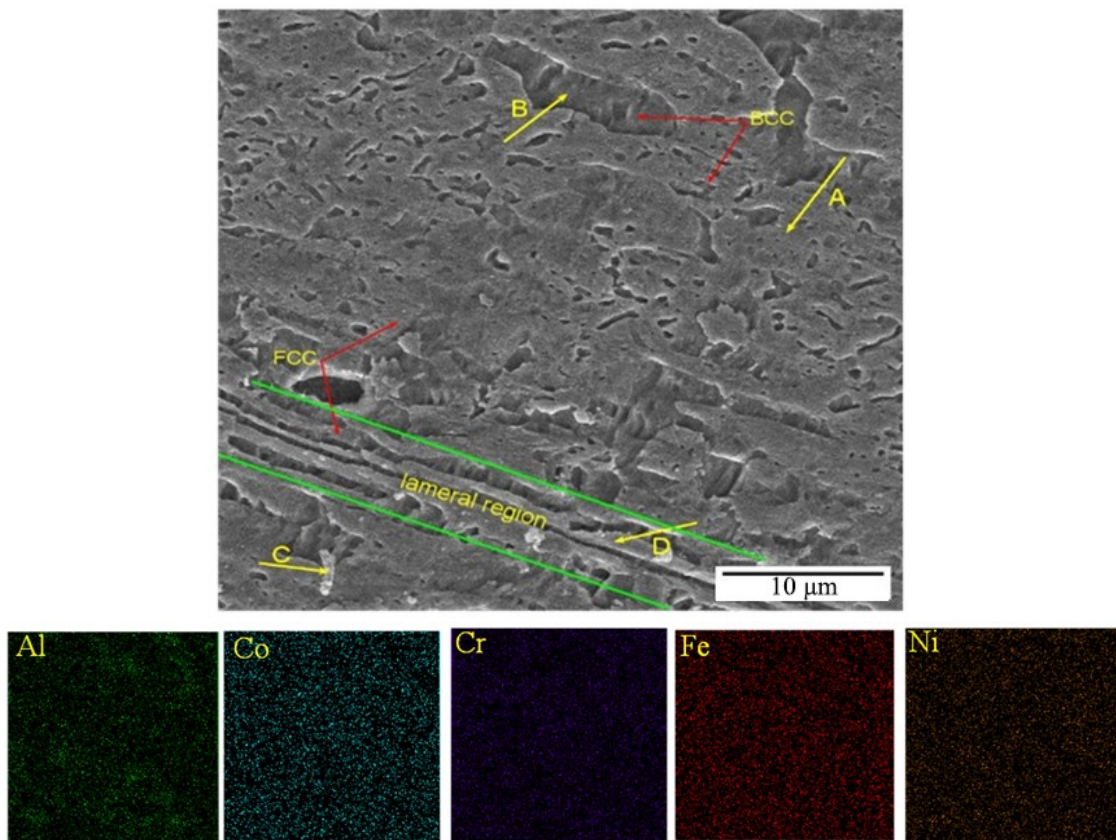

Fig. 2. SEM microstructure image of high entropy alloy AlCoCrCoFeNi$_{2.1}$ after 60% cold rolling.

Table 3. EDS analysis of marked points on Fig. 2

Point	Al	Co	Cr	Fe	Ni
A	6.77	18.69	19.29	19.48	35.76
B	18.12	12.88	8.70	11.37	48.93
C	8.07	18.17	18.60	18.07	37.09
D	11.33	17.23	17.24	17.36	36.83

Fig. 3 shows the X-ray pattern results for the as-cast and cold-rolled samples. As mentioned before, this alloy consists of two phases, FCC and BCC, which are shown in the figure. The XRD results also show that there is no peak shifting or new phase formation after cold rolling, however the intensity of the peaks in the cold rolled sample decreases compared to the as-cast sample. According to the image, the intensity of the FCC phase is clearly higher than that of the BCC phase, which implies that the L12 phase is the dominant phase in this alloy. In the as-cast sample, the peaks corresponding to the B2 phase are seen, while in the 60% cold rolled sample, these peaks are not seen, which may be related to the reduction in the size of the B2 phase.

The results of the shear-punch test showed that both as-cast and 60% cold-rolled samples have significant strength. The curves obtained from the shear-punch test for both cast and 60% cold-rolled samples at ambient temperatures and a speed of 0.2 mm/min are shown in Fig. 3. As shown in Table 3, the yield shear strength and final shear strength for the as-cast sample show the values of 204 and 269, that implies this alloy shows good strength and flexibility in the as-cast state that can be attributed to the eutectic solidification of the alloy, which occurs at a certain solidification temperature, and as a result, defects segregation and the formation of shrinkage cavities during solidification are minimized [7].
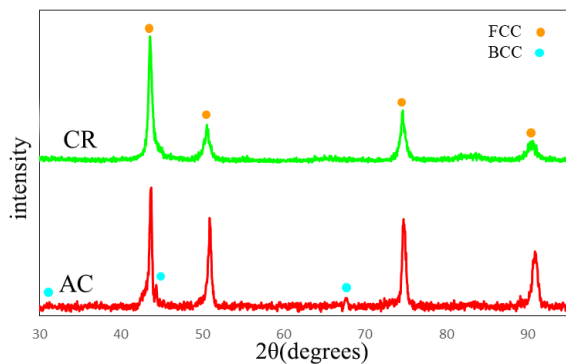
Table 3. Values of shear yield strength and ultimate shear strength for as-cast and 60% cold rolled samples

Sample	Ultimate shear strength	Yield shear strength
AC	269±9	214±10
60%CR	317±8	294±9

After 60% of cold rolling process, yield shear strength and ultimate shear strength increased to 294 and 317, respectively. Cold rolling process increases the density of dislocations and shear bands and creates a fine-grained nanostructure [18]. Cold rolling applies a compressive stress to the sample, this compressive stress causes the modification of the microstructure and the reduction or elimination of casting defects such as shrinkage cavities or other pores that are caused by the casting process. Hence, by reducing these defects, the strength of the alloy also increases after cold rolling. In addition, cold rolling reduces the grain size and increases the grain boundary area. With the increase of the grain boundaries, the movement of dislocations requires more stress, which causes an increase in yield and ultimate shear strength in the cold-rolled sample.

The average hardness for the cold rolled sample is 401 Vickers, which is about 14% higher than the as-cast sample with a hardness of 352 Micro granulation and increasing the density of grain boundaries makes it difficult for the dislocations to cross the grain boundary and as a result increases the hardness of the alloy.
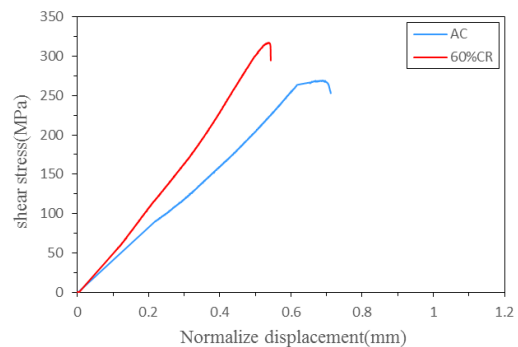

Fig. 3. X-ray pattern results for both cast and 60% cold rolled samples.

Fig. 4. Shear-punch test curves of as-cast and cold-rolled samples.

Table 4. Hardness values for the as-cast and cold-rolled samples

As-cast	Cold-rolled
352±5	401±7

4. Conclusion

- The high entropy alloy $AlCoCrFeNi_{2.1}$ in the as-cast state shows the eutectic microstructure and two phases of L12 (FCC) and B2 (BCC).

- After 60% cold rolling, there is no change in the phase structure of the alloy and the B2 phase particles are stretched in the direction of rolling.

- After applying cold rolling on the alloy, there was no difference in the distribution of elements in the two samples.

- After 60% of cold rolling, the shear strength and hardness increase significantly compared to the as-cast state. The yield strength and ultimate shear strength in the cast sample were 214 and 269 MPa, respectively, which increased to 294 and 317 MPa after 60% cold rolling, and the hardness of the alloy increased from 352 in the cast state to 417 Vickers after cold rolling.

- Cold rolling introduces a compressive stress to the sample, which causes the correction of the microstructure and the casting defects such as holes and pores are reduced, it also causes the reduction of the grain size and therefore the increase of the grain boundary. Microstructural modification and reduction of casting defects as well as reduction of grain size have increased the shear strength and micro-hardness of the cold-rolled sample.

Conflict of Interests

The authors declare no conflict of interest in this research.

Funding

5. Reference

[1] Shewmon, P. G., Lorig, C. H., Gill, C. B., & Charles, J. A. (2018). Metallurgy. *Encyclopedia Britannica, 26*.

[2] Murtu, B. S., Yeh, J. W., & Ranganathan, S. (2014). *High-entropy alloys* (1st ed.). Butte rwoth-Heinemann: Elsevier.

[3] Meyers M. A., & Chawla K. K. (2008). *Mechanical behavior of materials*. Cambridge University Press.

[4] Ritchie, R. O. (2011). The conflicts between strength and toughness. *Nature Materials*, *10*(11), 817-822. https://doi.org/10.1038/nmat3115

[5] Yeh, J. W., Chen, S. K., Lin, S. J., Gan, J. Y., Chin, T. S., Shun, T. T., Tsau, C.H & Chang, S. Y. (2004). Nanostructured high-entropy alloys with multiple principal elements: novel alloy design concepts and outcomes. *Advanced Engineering Materials*, 6(5), 299-303. https://doi.org/10.1002/adem.200300567

[6] Davis, J. R. (1990). *Metals handbook*. ASM International.

[7] Ayrenk, A. (2020). *Synthesis and development of refractory high entropy alloys* [Master's Thesis, Çankaya University http://hdl.handle.net/20.500.12416/4904

[8] Zhang, Y., Zuo, T. T., Tang, Z., Gao, M. C., Dahmen, K. A., Liaw, P. K., & Lu, Z. P. (2014). Microstructures and properties of high-entropy alloys. *Progress in Materials Science*, *61*, 1-93. https://doi.org/10.1016/j.pmatsci.2013.10.001

[9] Pickering, E. J., & Jones, N. G. (2016). High-entropy alloys: a critical assessment of their founding principles and future prospects. *International Materials Reviews*, *61*(3), 183-202. https://doi.org/10.1080/09506608.2016.1180020

[10] Miracle, D. B., & Senkov, O. N. (2017). A critical review of high entropy alloys and related concepts. *Acta Materialia*, *122*, 448-511. https://doi.org/10.1016/j.actamat.2016.08.081

[11] Tsai, M. H., & Yeh, J. W. (2014). High-entropy alloys: a critical review. *Materials Research Letters*, *2*(3), 107-123. https://doi.org/10.1080/21663831.2014.912690

[12] Guo, S., Ng, C., Lu, J., & Liu, C. T. (2011). Effect of valence electron concentration on stability of fcc or bcc phase in high entropy alloys. *Journal of Applied Physics*, *109*(10). https://doi.org/10.1063/1.3587228

[13] Chang, X., Zeng, M., Liu, K., & Fu, L. (2020). Phase engineering of high-entropy alloys. *Advanced Materials*, *32*(14), 1907226. https://doi.org/10.1002/adma.201907226

[14] Liao, Y., & Baker, I. (2008). Microstructure and room-temperature mechanical properties of $Fe_{30}Ni_{20}Mn_{35}Al_{15}$. Materials Characterization, 59(11), 1546-1549. https://doi.org/10.1016/j.matchar.2008.01.017

[15] Baker, I., Wu, M., & Wang, Z. (2019). Eutectic/ eutectoid multi-principle component alloys: a review. *Materials Characterization*, *147*, 545-557. https://doi.org/10.1016/j.matchar.2018.07.030

[16] Lei, Z., Wu, Y., He, J., Liu, X., Wang, H., Jiang, S., Gu, L., Zhang, Q., Gault, B., Raabe, D. & Lu, Z. (2020). Snoek-type damping performance in strong and ductile high-entropy alloys. *Science Advances*, *6*(25), eaba7802. https://doi.org/10.1126/sciadv.aba7802

[17] Lu, Y., Dong, Y., Guo, S., Jiang, L., Kang, H., Wang, T., Wen, B., Wang, Z., Jie, J., Cao, Z., Ruan, H & Li, T. (2014). A promising new class of high-temperature alloys: eutectic high-entropy alloys. *Scientific Reports*, *4*(1), 6200. https://doi.org/10.1038/srep06200

[18] Lu, Y., Jiang, H., Guo, S., Wang, T., Cao, Z., & Li, T. (2017). A new strategy to design eutectic high-entropy alloys using mixing enthalpy. *Intermetallics*, *91*, 124-128. https://doi.org/10.1016/j.intermet.2017.09.001

[19] Jiang, H., Zhang, H., Huang, T., Lu, Y., Wang, T., & Li, T. (2016). Microstructures and mechanical properties of Co2MoxNi2VWx eutectic high entropy alloys. *Materials & Design*, *109*, 539-546. https://doi.org/10.1016/j.matdes.2016.07.113

[20] Lu, Y., Gao, X., Jiang, L., Chen, Z., Wang, T., Jie, J., Kang, H., Zhang, Y., Guo, S., Ruan, H. and Zhao, Y., Cao, Z & Li, T. (2017). Directly cast bulk eutectic and near-eutectic high entropy alloys with balanced strength and ductility in a wide temperature range. *Acta Materialia*, *124*, 143-150. https://doi.org/10.1016/j.actamat.2016.11.016

[21] Bhattacharjee, T., Wani, I. S., Sheikh, S., Clark, I. T., Okawa, T., Guo, S., Bhattacharjee, P.P.& Tsuji, N. (2018). Simultaneous strength-ductility enhancement of a nano-lamellar AlCoCrFeNi$_{2.1}$ eutectic high entropy alloy by cryo-rolling and annealing. *Scientific Reports*, *8*(1), 3276. https://doi.org/10.1038/s41598-018-21385-y

[22] Wang, Y., Chen, W., Zhang, J., & Zhou, J. (2021). A quantitative understanding on the mechanical behavior of AlCoCrFeNi$_{2.1}$ eutectic high-entropy alloy. *Journal of Alloys and Compounds*, *850*, 156610. https://doi.org/10.1016/j.jallcom.2020.156610

[23] Vikram, R. J., Murty, B. S., Fabijanic, D., & Suwas, S. (2020). Insights into micro-mechanical response and texture of the additively manufactured eutectic high entropy alloy AlCoCrFeNi$_{2.1}$. *Journal of Alloys and Compounds*, *827*, 154034. https://doi.org/10.1016/j.jallcom.2020.154034

[24] Gao, X., Lu, Y., Zhang, B., Liang, N., Wu, G., Sha, G., Sha, G., Liu, J. & Zhao, Y. (2017). Microstructural origins of high strength and high ductility in an AlCoCrFeNi$_{2.1}$ eutectic high-entropy alloy. *Acta Materialia*, *141*, 59-66. https://doi.org/10.1016/j.actamat.2017.07.041

[25] Shukla, S., Wang, T., Cotton, S., & Mishra, R. S. (2018). Hierarchical microstructure for improved fatigue properties in a eutectic high entropy alloy. *Scripta Materialia*, *156*, 105-109. https://doi.org/10.1016/j.scriptamat.2018.07.022